Inorg. Chem. **2007**, *46*, 10287–10293

Novel Inorganic–Organic Hybrid Fluorescence Chemosensor Derived from SBA-15 for Copper Cation

Ling Gao,[†] Jian Qiang Wang,[‡,§] Li Huang,[‡,§] Xiao Xing Fan,[‡] Jian Hua Zhu,*[,†] Ying Wang,*[,‡,§] and Zhi Gang Zou[‡]

Key Laboratory of Mesoscopic Chemistry, College of Chemistry and Chemistry Engineering, Eco-materials and Renewable Energy Research Center, and School of Chemistry and Chemical Engineering, Nanjing University, Nanjing 210093, China

Received May 6, 2007

A novel mesoporous SBA-15 type of hybrid material (3-trimethoxysilylpropyl)[4-(2-hydroxyphenyl)methylene] benzenesulfonamide (Schiff-SBA-15) has been obtained by co-condensation of tetraethyl orthosilicate and the organosilane, and the result of XRD confirms the order hexagonal structure of the composite. This hybrid mesoporous material is fluorescent-active, exhibiting high selectivity for sensing Cu^{2+} in polar solution. The remarkable fluorescence quenching in emission spectrum upon the addition of Cu^{2+} is attributed to the intramolecular charge transfer after the formation of a coordinate complex of a large conjugate system and Cu^{2+} ions.

Introduction

Organically functionalized mesoporous siliceous materials have generated a great deal of interest in the fields of catalysis, adsorption,[1−6] and sensors[7] due to their high surface areas and large ordered pores ranging from 2 to 50 nm with narrow size distributions. Among these potential applications, trapping heavy metal ion by the hybrid material is crucial for environmental cleanup.[8] For this purpose, a variety of bulky organic functional molecules such as tetraazacyclotetradecane, izocyanurate, and Schiff-base were grafted or incorporated inside the channel of mesoporous materials.[9−11] The design and synthesis of these innovative hybrid mesoporous materials for heavy metal ions detection are of considerable interest and opens up an extraordinary field of investigation.[12] Cu^{2+} is a significant environmental pollutant and an essential trace element in biological systems,[13] so the design and synthesis of chemosensors for Cu^{2+} constitute a very active area of research as a result of the demand for more sensitive and selective chemosensors. Although chromogenic sensors have attracted much attention due to their capability to detect analytes by the naked eye without resorting to any expensive instruments[14] and fluorescence is also popular for its in-real-time detection and sensitivity,[15,16] the synthetic Cu^{2+} selective fluoroionophores so far reported[17,18] suffer from low sensitivity and, in general, higher concentrations of interfering metal ions disturb the selectivity toward Cu^{2+}.

In these systems, the solid support lends stability while the chromophore fluorophore provides the necessary binding site for the analyte, leading to changes in its properties such

* To whom correspondence should be addressed. E-mail: jhZhu@netra.nju.edu.cn (J.H.Z.); wangy@netra.nju.edu.cn (Y.W.).
[†] Key Laboratory of Mesoscopic Chemistry, College of Chemistry and Chemistry Engineering.
[‡] Eco-materials and Renewable Energy Research Center.
[§] School of Chemistry and Chemical Engineering.

(1) Lee, B.; Kim, Y.; Lee, H.; Yi, J. *Microporous Mesoporous Mater.* **2001**, *50*, 77.
(2) Liu, K.; Hidajat, K.; Kawi, S.; Zhao, D. Y. *Chem. Commun.* **2000**, 1145.
(3) Hossain, K. Z.; Mercier, L. *Adv. Mater.* **2002**, *14*, 1053.
(4) Lee, H.; Yi, J. *Sep. Sci. Technol.* **2001**, *36*, 2433.
(5) Lim, M. H.; Stein, A. *Chem. Mater.* **1999**, *11*, 3285.
(6) Ho, K. Y.; Mckay, G.; Yeung, K. L. *Langmuir* **2003**, *19*, 3019.
(7) Zhou, H. S.; Sasabe, H.; Honma, I. *J. Mater. Chem.* **1998**, *8*, 515.
(8) Stein, A.; Melde, B. J.; Schroden, R. C. *Adv. Mater.* **2000**, *12*, 1403.
(9) Corriu, R. J. P.; Mehdi, A.; Reyé, C.; Thieuleux, C. *Chem. Commun.* **2002**, 1382.
(10) Olkhovyk, O.; Jaroniec, M. *J. Am. Chem. Soc.* **2005**, *127*, 60.
(11) Corriu, R. J. P.; Lancelle-Beltran, E.; Mehdi, A.; Reyé, C.; Brandès, S.; Guilard, R. *Chem. Mater.* **2003**, *15*, 3152.
(12) (a) Hirano, T.; Kikuchi, K.; Urano, Y.; Higuchi, T.; Nagano, T. *Angew. Chem., Int. Ed.* **2000**, *39* (6), 1052. (b) Panchard, M. S.; Huber, R.; Renault, M.; Maas, H.; Pansu, R.; Calzaferri, G. *Angew. Chem., Int. Ed.* **2001**, *40*, 2839.
(13) (a) Kramer, R. *Angew. Chem., Int. Ed.* **1998**, *37*, 772. (b) Zheng, Y.; Orbulescu, J.; Ji, X.; Andreopoulos, F. M.; Pham, S. M.; Leblanc, R. M. *J. Am. Chem. Soc.* **2003**, *125*, 2680. (c) Kaur, S.; Kumar, S. *Tetrahedron Lett.* **2004**, *45*, 5081.
(14) Anzenbacher, J. P.; Try, A. C.; Miyaji, H.; Jursikova, K.; Lynch, V. M.; Marquez, M.; Sessler, J. L. *J. Am. Chem. Soc.* **2000**, *122*, 10268.
(15) Gale, P. A.; Twyman, L. J.; Handlin, C. I.; Sessler, J. L. *Chem. Commun.* **1999**, 1851.
(16) Han, M. S.; Kim, D. H. *Angew. Chem., Int. Ed.* **2002**, *41*, 3809.
(17) Wirnsberger, G.; Scott, B. J.; Stucky, G. D. *Chem. Commun.* **2001**, 119.
(18) Mercier, L.; Pinnavaia, T. J. *Adv. Mater.* **1997**, *9*, 500.

10.1021/ic7008732 CCC: $37.00
Published on Web 10/31/2007

Scheme 1. Synthesis Scheme of Hybrid Chemosensor SBA-15-Schiff: (a) Ether, 273 K; (b) TEOS, P123; (c) Ethanol, Salicylal, Room Temperature

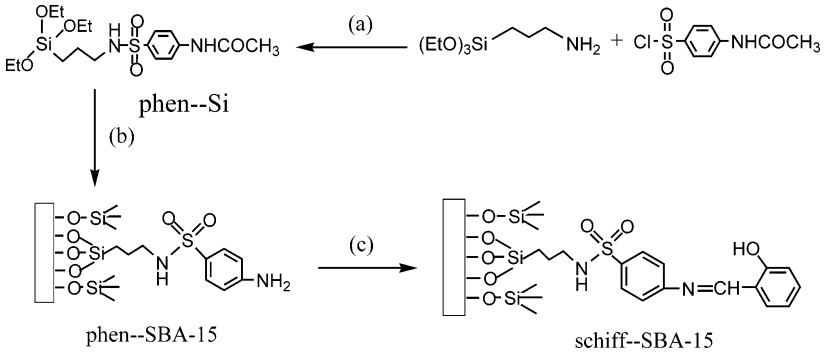

as color, fluorescence, and nonlinear optical behavior. Among the inorganic host materials, mesoporous materials have attracted much attention for electronic and optical applications due to their high surface area, uniform porosity, and low absorption and emission in the visible spectrum, making them suitable host materials for sensing molecules or ions.[19,20] Recently, we reported a technique for encapsulating a small organic molecular SC (4-chloroaniline-*N*-salicylidene) into the channel of amine-functionalized SBA-15 to form a zinc chemosensor.[21]

The co-condensation method is one of the two approaches, grafting and direct synthesis, to surface modification that was first reported in 1996.[22,23] This method allows the surface modification of the mesoporous materials in a single step by copolymerization of organosilane with silica or organosilica precursors in the presence of a surfactant, enabling a higher and more homogeneous surface coverage of organosilane functionalities than the grafting method.[24,25] In this paper, we utilize the direct synthesis method to create the Schiff base fluorophore-functionalized mesostructure hybrid material, and this new procedure involves a one-step synthetic strategy based on the co-condensation of tetraethoxysilane (TEOS) and the organosilane phen-Si (Scheme 1). The block copolymer P123 is used as the surfactant template and phen-Si here is the source of organic groups. The new fluorescence sensor Schiff-SBA-15 displayed an excellent selectivity for Cu^{2+} in an ethanol−water mixed solution. To the best of our knowledge, there is no report on the assembly of a Cu^{2+}-selective chemosensor based on mesoporous material SBA-15 by using the co-condensation method. XRD, N_2 adsorption−desorption, UV−vis, FT-IR, and fluorescence spectroscopy are employed to characterize the obtained hybrid materials.

Experimental Section

Reagent and Chemicals. Pluronic P123, an ethylene oxide (EO)/propylene oxide (PO) triblock copolymer with composition EO_{20}-$PO_{70}EO_{20}$ and with an average molecular weight of 5800, was purchased from Aldrich. Tetraethyl orthosilicate (TEOS), the silica source, (aminopropyl)triethoxysilane (APTES), salicylaldehyde, acetanilide, and chlorosulfonic acid were procured from Nanjing Chemical Reagent Company (China). $Cu(CH_3COO)_2$ and the other metal salts were provided by Shanghai Fourth Chemical Reagent Company (China). All of the reagents and solvents were of analytical reagent grade and used as received.

Synthesis of the Organosilane phen-Si. Five grams of acetanilide is dissolved into 12 mL of chlorosulfonic acid at room temperature. The mixture was decanted into ice water (100 g), then the white suspension was filtered and dissolved into ether at once, and the water from the delivery flask was thrown away. (3-Aminopropyl) triethoxysilane (8.6 g) and triethylamine (3 mL) were added to the ether solution and the mixture was then stirred at 273 K for 5 h. The final white suspension was filtered and dried at room temperature under vacuum. ^{1}H NMR ($CDCl_3$, 300 MHz): δ_H 0.45 (m, 2 H, CH_2Si), 1.2 (m, 2 H, CH_2), 3.06 (s, 3 H, OMe), 3.36 (s, 15 H, OEt), 3.69 (t, 2 H, CH_2N), 6.97 (s, 1 H, NH), 7.03 (s, 4 H, Ar), 7.74 (s, 1 H, NH). IR data: υ_{max} (KBr pellets)/cm^{-1} 3359 (br, CH, arom), 3100 (br, CH, arom), 2980 (m, C−H), 2943 (m, C−H), 1530 (s, HN−S═O), 1319 (s, S═O, arom), 1084 (m, Si−O, arom).

Preparation of Hybrid Mesoporous Materials Schiff-SBA-15. The preparation was carried out according to the literature.[26] The mixture of P123 (2.0 g, 0.034 mmol), 2.0 M of HCl solution (60 mL, 100 mmol), and H_2O (15 mL, 0.83 mol) was heated at 313 K. To this clear solution, TEOS (4.25 g, 20.4 mmol) and phen-Si (200 mg, 0.63 mmol) were first dissolved in a small volume of methanol and then added into the surfactant solution since the presence of a suitable amount of methanol in the system might increase the orderliness of the mesoporous materials compared with a purely aqueous system.[27] The mixture was stirred at 313 K for 24 h, then transferred into a Teflon bottle sealed in an autoclave, and heated to 373 K for another 24 h.[28] The product was recovered by filtration and air-dried. To remove the surfactant, 1.0 g of as-synthesized material was twice stirred in 150 mL of ethanol and 1.0 g of 37% HCl aqueous solution at 333 K for 6 h. The resulting surfactant-removed solid was filtered and washed with distilled water and ethanol, and the product was denoted as phen-SBA-15. After being dried in air, the product was stirred in the salicylaldehyde ethanol solution, and a bright yellow precipitate emerged after 3 min of stirring. The reaction was maintained at room temperature

(19) Brasola, E.; Mancin, F.; Rampazzo, E.; Tecilla, P.; Tonellato, U. *Chem. Commun.* **2003**, 3026.
(20) Métivier, R.; Leray, I.; Lebeau, B.; Valeur, B. *J. Mater. Chem.* **2005**, *15*, 2965.
(21) Gao, L.; Wang, Y.; Wang, J. Q.; Huang, L.; Shi, L. Y. *Inorg. Chem.* **2006**, *45*, 6844.
(22) Burkett, S. L.; Sims, S. D.; Mann, S. *Chem. Commum.* **1996**, 1367.
(23) Macquaire, J. D. *Chem. Commun.* **1996**, 1961.
(24) Richer, R.; Mercier, L. *Chem. Commun.* **1998**, 1775.
(25) Macquaire, J. D.; Jackson, D. B.; Mdoe, J. E. G.; Clark, J. H. *New. J. Chem.* **1999**, *23*, 539.
(26) Huh, S.; Wiench, J. W.; Yoo, J.; Pruski, M.; Lin, W. S. Y. *Chem. Mater.* **2003**, *15*, 4247.
(27) (a) Moller, K.; Bein, T.; Fischer, R. X. *Chem. Mater.* **1999**, *11*, 665. (b) Anderson, M. T.; Martin, J. E.; Odinek, J. G.; Newcomer, P. P. *Chem. Mater.* **1998**, *10*, 1490.
(28) (a) Valeur, B.; Leray, I. *Coord. Chem. Rev.* **2000**, *205*, 3. (b) Silva, A. P.; Fox, D. B.; Huxley, A. J. M.; Moody, T. S. *Coord. Chem. Rev.* **2000**, *205*, 41.

for 4 h and then the product was filtered, washed with ethanol, air-dried, and denoted as Schiff-SBA-15.

Instruments and Spectroscopic Measurements. The ^{1}H NMR experiments were operated on a set of Bruker DPX-300 spectrometers at 298 K, and $CDCl_3$ was used as the solvent. All chemical shifts are reported in the standard δ notation of ppm; positive chemical shifts are denoted to higher frequency from the given reference. X-ray powder diffraction (XRD) measurements were performed with a Brucker AXS D8 ADVANCE diffractometer with Cu Kα radiation at 40 kV and 20 mA. Nitrogen adsorption/desorption isotherms were measured at the liquid nitrogen temperature, using a Nova 1000 analyzer. Samples were degassed at 373 K overnight before measurements. Specific surface areas were calculated using the BET method. Pore size distributions were evaluated from the desorption branches of the nitrogen isotherms using the BJH method. The IR spectra were obtained on a Bruker Vector 22, and the sample was mixed with KBr at a ratio of 3:97 (w/w) and then pressed as a thin disk for testing. UV−vis diffuse-reflectance absorption spectra of the opaque powders were recorded under ambient conditions from 200 to 600 nm on a Shimadzu UV-2401PC spectrophotometer adapted with a praying mantis attachment and use of $BaSO_4$ as the reference. Steady-state fluorescence spectra were acquired on a Varian-Cary Eclips spectrofluorometer at room temperature. All spectrophotometric titrations were performed with a suspension of the sample dispersed in a ethanol/water (9:1, v/v) solution (pH 7.0), and then the sample was brought into a quartz cell for measurement. Combustion chemical analyses (C, H, and N) of the silicates containing organic material were carried out in a CHNO− Rapid (Germany) elemental analyzer. Curve fitting and data analysis of the Stern−Volmer quenching relationships were completed in Microsoft Excel 2000, using the Solver plug-in application and minimizing the sum of the square of the residuals.

Results and Discussion

Synthesis and Characterization. Organic ligand phen-Si bearing the $Si(OEt)_3$ group was synthesized according to the procedure for the synthesis of (3-trimethoxysilylpropyl)-[4-(2-hydroxyphenyl)methylene] benzenesulfonamide (Schiff-SBA-15), as mentioned in the Experimental Section. As for the imprinting technique used in our experiment, the phen-Si plays the role of connecting the organic moiety in the silica matrix during the co-condensation process by covalent linking to the matrix,[29] and the −C═N− bond combined by stirring the product phen-SBA-15 in the salicylaldehyde ethanol solution. Thus, the surfactant-extracted product phen-SBA-15 was stirred in salicylaldehyde ethanol solution for obtaining the Schiff base. The hybrid mesoporous product, Schiff-SBA-15, was obtained as outlined in Scheme 1.

Figure 1 illustrates the X-ray diffraction (XRD) patterns of bare SBA-15 and the hybrid materials phen-SBA-15 and Schiff-SBA-15. The samples of phen-SBA-15 and Schiff-SBA-15 show three peaks, one intense diffraction peak corresponding to d_{100} spacing and two weak higher order reflections, which can be indexed as the (100), (110), (200) reflections of the hexagonal symmetry lattice of SBA-15 material. These results suggest the presence of a periodic arrangement of hexagonal geometry channels in both hybrid materials.

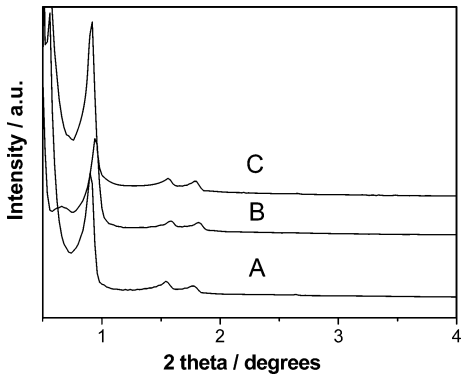

Figure 1. Low-angle XRD patterns of (A) SBA-15, (B) Schiff-SBA-15, and (C) phen-SBA-15.

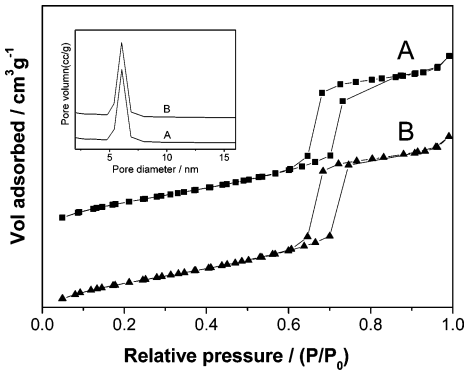

Figure 2. N_2 adsorption−desorption isotherms of (A) phen-SBA-15 and (B) Schiff-SBA-15. The insert shows the BJH pore size distributions determined from the adsorption branch. The ordinates of A in Figure 2 are offset by 220 m^3 g^{-1}, while the ordinates of A in the insert of the figure are offset by 1.0 cm^3 g^{-1}.

Figure 2 depicts the N_2 adsorption−desorption isotherms of phen-SBA-15 and Schiff-SBA-15 samples. The type IV isotherms, with a clear H1-type hysteresis loop at high relative pressure that is a characteristic of mesoporous materials (pore diameters 2−50 nm), provide further proof on the mesoporous structure of two hybrid materials.[30,31] The insert in Figure 2 shows the BJH pore size distribution plots of two hybrid materials in which an average BJH pore size is measured from the adsorption branch. The pore size distributions are narrow in the range of 5−8 nm (centered at 6.4 nm) for both phen-SBA-15 and Schiff-SBA-15 samples, indicating that the mesostructure of SBA-15 are remained after co-condensation of and grafting of Schiff ligands.

Table 1 summarizes the textural parameters of phen-SBA-15 and Schiff-SBA-15 samples. Anchoring salicylaldehyde moiety onto phen-SBA-15 affects the BET specific surface area and porosity of the composite, giving additional proof of the inner channel immobilization of Schiff base fluorescent chromophore. The BET surface area of phen-SBA-15 sample declines from 549 to 539 m^2 g^{-1} due to the linkage of salicylaldehyde moiety. Likewise, the pore volume of phen-SBA-15 also slightly decreases from 0.849 to 0.843 cm^3 g^{-1} concomitant with the pore size changing from 0.625 to 0.618

(29) Luo, Y.; Lin, J. *Microporous Mesoporous Mater.* **2005**, *86*, 23.
(30) Jia, M.; Seifert, A.; Berger, M.; Giegengack, H.; Schulze, S.; Thiel, W. R. *Chem. Mater.* **2004**, *16*, 877.
(31) Jaroniec, M.; Solovyov, L. A. *Langmuir.* **2006**, *22*, 6757.

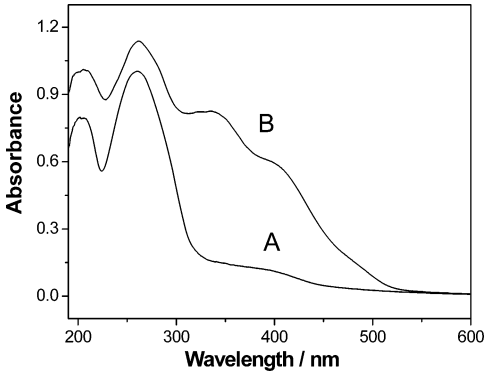

Figure 3. UV−vis spectra of (A) phen-SBA-15 and (B) Schiff-SBA-15.

Table 1. Textural Properties of the phen-SBA-15 and Schiff-SBA-15

sample	S_{BET} (m^2/g)	V_p (cm^3/g)	D_p (nm)
phen-SBA-15	549	0.849	6.25
Schiff-SBA-15	539	0.843	6.18

nm. Such relative small shrinkages in the structural parameters of Schiff-SBA-15 originate probably from the small size of salicylaldehyde moiety. Moreover, the quantity of grafting organic moiety is very small (the phenyl functional groups are only 3 mol % in Si−O framework), which probably could not result in an obvious reduction in the texture parameters from phen-SBA-15 to Schiff-SBA-15.

Both XRD and N_2-sorption analyses demonstrate that the hexagonal arrangement of the mesopore is not affected during the co-condensation process. Compared with phen-SBA-15, the slight decrease of the surface area and pore width observed in Sciff-SBA-15 sample may be due to a small increased organic functional group after the Schiff base moiety formation process. Collectively, the XRD patterns also suggest not only a significant degree of short-range ordering of the structure and well-formed hexagonal pore arrays of the samples but also the maintenance of the structural ordering of the synthesized adsorbent after organosilane functionalization.[32]

Figure 3 depicts the UV−vis diffuse reflectance spectra of phen-SBA-15 and Schiff-SBA-15 in which two new broad absorption bands emerge in that of Schiff-SBA-15 with the center at about 338 and 406 nm (curve B in Figure 3). These bands are characteristic of Schiff base,[21] originating from the typical electronic transition of an aromatic ring and −C═N− conjugate system in a molecule of Schiff base;[33] their appearance indicates that the Schiff base is composed and the salen group is covalently grafted to the silica after the co-condensation process. The FT-IR spectrum also discloses the grafting of salen group to the silica (characteristic C═N stretching at 1634 cm^{-1}).[28] Elemental analysis demonstrates that content of the Schiff base ligand is about 0.42 mmol/g.

The sensing capability of Schiff-SBA-15 was evaluated against a series of representative metal ions at first, including alkali, alkaline earth, and heavy metal ions in ethanol−water

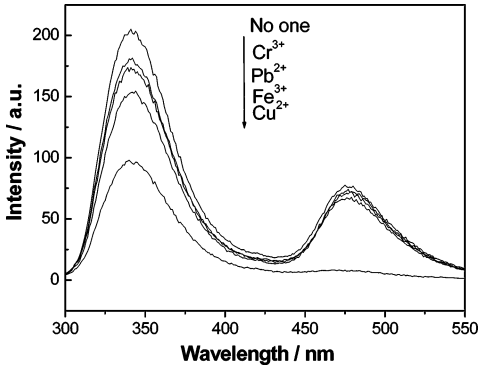

Figure 4. Fluorescence spectra of Schiff-SBA-15 in the presence of different metal ions (5.0×10^{-5} M).

solution for which the very diluted solutions (Schiff-SBA-15 = 0.1 g/L, corresponding to a concentration of the Schiff base fluorophore of 4.0×10^{-5} M), were used. Schiff-SBA-15 exhibits a very intense fluorescence in the mixed solution as shown in Figure 4. The addition of alkaline metal ions such as Na^+ and K^+ into the ligand does not change the fluorescence intensity, suggesting the nonsensitivity of fluorophore to the presence of alkali metal ions with a unique implication; therefore, there will be no interference from such metal ions. Addition of Ca^{2+} or Mg^{2+} into the solution does not generate change in the fluorescence intensity either. With the use of transition metal and heavy metal ions, the fluorescence is slightly quenched by the addition of Cr^{3+}, Pb^{2+}, and Fe^{3+}, respectively, whereas there is nearly no response to some other cations such as Ag^+, Ni^{2+}, Mn^{2+}, Zn^{2+}, and Co^{2+}. That means, little response in fluorescent spectra, upon addition of these cations, is observed. However, the fluorescence of Schiff-SBA-15 is significantly quenched by Cu^{2+}, especially at a much higher F_0/F (F_0/F = 10.5, $\lambda_{max(em)}$ = 476 nm, F_0 is the initial fluorescence intensity before the metal addition and F is the intensity after the metal addition). Obviously, a significant change in color from light yellow to achromatism is also observed. The fluorescent emission at 476 nm is nearly completely quenched, mirroring the high selectivity of Schiff-SBA-15 for Cu^{2+}.[34]

Figure 5 illustrates the UV−vis absorption spectra of Schiff-SBA-15 solution containing different concentrations of Cu^{2+}. There are two characteristic bands, 213 and 259 nm, which are useful as the excitation wavelength for the subsequent fluorescence measurements. These two peaks are the features of the conjugated system,[35] and they involve the lone pair electron of N in the −C═N− groups and can be ascribed to a $\pi-\pi^*$ transition.[36] Addition of Cu^{2+} to the solution of Schiff-SBA-15 gradually enlarges both of the bands, resulting from the protonation of the hydroxy moiety to enhance the intramolecular charge-transfer (ICT) character of the molecule. The enhancement of these two peaks can be explained by extension of the conjugated system resulting from the presence of an additional Cu^{2+} because the

(32) Kang, T.; Park, Y.; Choi, K.; Lee, J. S.; Yi, J. J. *Mater. Chem.* **2004**, *14*, 1043.
(33) (a) Parker, C. A.; Rees, W. T. *Analyst* **1960**, *85*, 587. (b) Wang, X. Q.; Lin, S. K.; Chan, C. C.; Cheng, S. *J. Phys. Chem. B* **2005**, *109*, 1763. (c) Sutra, P.; Brunel, D. *Chem. Commun.* **1996**, 2485.
(34) Wirnsberger, G.; Scott, B. J.; Stucky, G. D. *Chem. Commun.* **2001**, 119.
(35) Kawamata, J.; Akiba, M.; Inagaki, Y. *Jpn. J. Appl. Phys.* **2003**, *42*, L17.
(36) Huang, J. H.; Wen, W. H.; Sun, Y. Y.; Chou, P. T.; Fang, J. M. *J. Org. Chem.* **2005**, *70*, 5827.

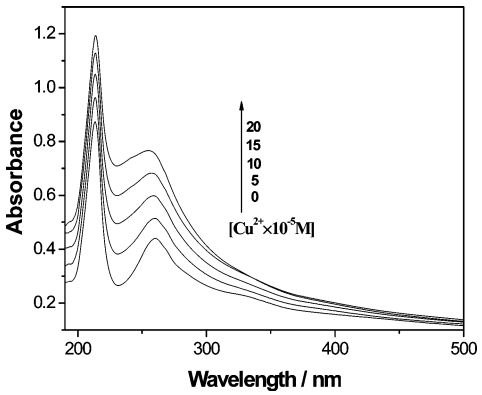

Figure 5. UV−vis spectra changes of Schiff-SBA-15 (0.1 g/L) upon addition of Cu^{2+} in ethanol/water (9:1 v/v).

conformation modification of the organic ligand occurs with complexation toward Cu^{2+} in solution. The coordination of Cu^{2+} to the entire large π-electron system consisting of a Schiff base-functionalized inner surface of SBA-15 may increase the rigidity of the π system. Yet this result can be considered as metal binding enhancing the electronic transition processes of the conjugated system.

The spectrum of Schiff-SBA-15 does not show any absorption above 350 nm. Once copper acetate is added, a remarkable increase in the absorption is observed in the range of 200−350 nm that rises with the increased concentration of Cu^{2+}. This band is significantly wider and attributed to a charge-transfer transition resulting from the displacement of the electron density from the donor amino group toward the acceptor metal ions.[37] Additionally, this phenomenon indicates that, in this solvent system, the hybrid material can provide strong sites for binding Cu^{2+}, and it is the cocondensation of the sensor components on the mesoporous surfaces that ensures the spatial proximity necessary to the communication between the subunits.[38]

Detection of Cu^{2+} by the Schiff-SBA-15 Sensor. Fluorescent techniques have been widely used to investigate the receptor−substrate interactions due to their high sensitivity.[39] In this work, the complexation behavior of Schiff-SBA-15 toward various cations is also assessed by fluorescence titration in the case of Schiff-SBA-15 in a mixture of ethanol/water solution. Figure 6 shows the fluorescence spectral changes of Schiff-SBA-15 solution with various concentrations of Cu^{2+} in which the fluorescence intensity is decreased upon the increase of Cu^{2+} concentrations. These results are consistent with the electronic transition changes in the absorption titration.[40]

For Schiff-SBA-15 itself, the emission maximum is situated at 343 and 478 nm, indicating that fluorescence comes from two species.[41,42] These bands are attributed to a charge-transfer (CT) transition resulting from the displacement of the electron density from the donor sulfonic group toward the acceptor imino group. Addition of Cu^{2+} leads to a dramatic decrease in the fluorescence intensity; it drops by 52% upon the initial addition [Cu^{2+}/fluorophore molar ratio 1:4] and the subsequent addition (Cu^{2+}/fluorophore molar ratio 1:2) causes a further drop by 65%. As the molar ratio increases to 1:1, the fluorescence is further dropped by 80% (Figure 6). There is a linear change in emission from 0 to 50 μM Cu^{2+} but, beyond this, the rate of quenching in the emission declines, and the F_0/F increases slightly indeed. The current condition involves the use of 0.1 g/L of hybrid material concentration, and the detection limit calculated as three times the standard deviation of the background noise is found to be 0.1 ppm.

Chart 1. Reaction of Schiff-SBA-15 with Cu^{2+} Ion

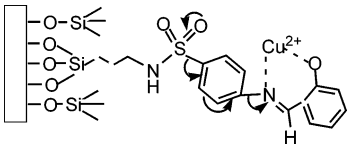

The fluorescence quenching at 478 nm provides the relevant structural information on the complexation of Cu^{2+} cations with Schiff-SBA-15. These results imply that Cu^{2+} is complexed with the organic fluorophore, strongly quenching the emission intensity, as shown in Chart 1. This is not surprising since Cu^{2+} has a particularly high thermodynamic affinity for typical N, O-chelate ligands among the more relevant transition metal ions.[43] The fluorophore here chelates with Cu^{2+} via its imino N and phenol O atoms after the addition of Cu^{2+} ions, especially the phenol group of fluorophore which undergoes deprotonation during the binding and plays an indispensable role in the affinity of Schiff-SBA-15 to Cu^{2+}.[44] Complexation of copper by the Schiff base moiety induces a charge transfer from the electron-donating site of sulfonic O to the accepter site imino N; the donor and acceptor moieties are connected by a benzene ring to form a conjugated scaffold. The binding of the accepter−donor molecule with Cu^{2+} ion at the acceptor site, forming MA-D, would enhance the acceptor strength to facilitate intramolecular charge transfer (ICT). Subsequently, the copper concentration can be determined by the measurement of the fluorescence intensity with a fluorimeter. Moreover, the inset in Figure 6 displays the plot of optical density at 476 nm versus Cu^{2+} concentration in solution. As shown in the plot, an approximate plateau is observed at a 1:1 molar ratio of organic ligand to cation guest, indicative of the formation of a 1:1 stoichiometrical complex in solution. Hence, the fluorescence is quenched completely upon coordination of Cu^{2+} ions, presumably through an intramolecular metal-to-fluorophore electron-transfer mechanism.

(37) Jérome, M.; Béatrice, D. N.; Suzanne, F. F.; Dominique, L.; René, M. *Inorg. Chem.* **2002**, *41*, 5002.
(38) Brasola, E.; Mancin, F.; Rampazzo, E.; Tecilla, P.; Tonellato, U. *Chem. Commun.* **2003**, 3026.
(39) (a) Tong, H.; Zhou, G.; Wang, L. X.; Jing, X. B.; Wang, F. S.; Zhang, J. P. *Tetrahedron Lett.* **2003**, *44*, 131. (b) Kubo, Y.; Tsukahara, M.; Ishihara, S.; Tokita, S. *Chem. Commun.* **2000**, 653. (c) Fabbrizzi, L.; Licchelli, M.; Rabaioli, G.; Taglietti, A. *Coord. Chem. Rev.* **2000**, *205*, 85.
(40) Zhou, L. L.; Hao, S.; Li, H. P.; Wang, H.; Zhang, X.; H.; Wu, S. K.; Lee, S. T. *Org. Lett.* **2004**, *6* (7), 1171.
(41) Hanaoka, K.; Kikuchi, K.; Kojima, H.; Urano, Y.; Probes, L. *Angew. Chem., Int. Ed.* **2003**, *42*, 2996.
(42) Gunnlaugsson, T.; MacóDnail, D. A.; Parker, D. *Chem. Commun.* **2000**, 93.
(43) Dujols, V.; Ford, F.; Czarnik, A. W. *J. Am. Chem. Soc.* **1997**, *119*, 7386.
(44) Krämer, R. *Angew. Chem., Int. Ed.* **1998**, *37* (6), 772.

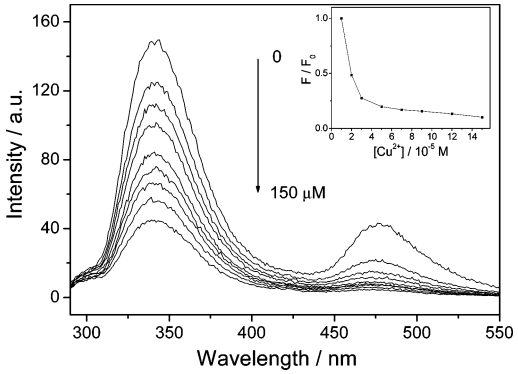

Figure 6. Emission spectrum (excitation at 268 nm) of Schiff-SBA-15 (0.1 g/L) in the presence of various concentrations of Cu^{2+}: $0-15 \times 10^{-5}$ M. Inset: Evolution of the normalized fluorescence F/F_0 of Schiff-SBA-15 ($\lambda_{em} = 478$) and as a function of Cu^{2+}.

Cu^{2+} also can quench the emission at 343 nm, as demonstrated in Figure 6. When the fluorescence of Schiff-SBA-15 is quenched upon Cu^{2+} binding, a blue shift of about 4 nm in the emission spectrum is observed, comparing with that of Cu^{2+}-free Schiff-SBA-15 solution. This blue shift is caused by the reduction of electron-donation ability of the sulfonic group of the fluorophore upon Cu^{2+} ion binding. In the case of Cu^{2+} binding, both energy transfer and electron transfer from the fluorophore to the complexed cation may be invoked to explain the observed fluorescence quenching. Such a blue-shift (12 nm) phenomenon is also observed in the emission spectra of dansyl fluorophores encapsulated in the pore structure of SBA-15 and interpreted in terms of the complexation effect of mercury on the photophysical properties of the hybrid material.[45]

The sensing ability of the functionalized material Schiff-SBA-15 is then mainly governed by the high affinity of the fluorophore ligand for Cu^{2+}. No specific effect of the surface is observed. The mesoporous silica can thus be considered as an inert matrix with respect to the complexation process, as already mentioned in recent works,[46] which allows one to control independently the different properties of the inorganic−organic hybrid system.

Interference with Other Cations. The effect of possible interfering cations such as K^+, Na^+, Ag^+, Ca^{2+}, Co^{2+}, Fe^{3+}, Mn^{2+}, Mg^{2+}, Al^{3+}, Ni^{2+}, Pb^{2+}, Cr^{3+}, and Zn^{2+} is examined. Titration of Schiff-SBA-15 with copper acetate in the presence of these interested ions at 50 μM respectively does not affect the luminescence emission as observed in the case of Cu^{2+} only (displayed in Figure 7), which represents that these ions have no effect in the presence or absence of Cu^{2+} ions. Therefore, these metal ions do not interfere in the estimation of Cu^{2+}. Figure 7 clearly discloses an extremely good selectivity for Cu^{2+} at low concentration against all other cations tested here.

Consequently, the new hybrid material Schiff-SBA-15 can be used as a chemosensor for the detection of different concentrations of Cu^{2+} with high selectivity.

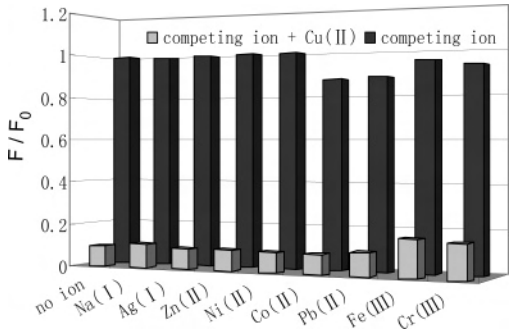

Figure 7. Normalized fluorescence response F/F_0 of Schiff-SBA-15 (0.1 g/L in ethanol/water solution) in the presence of various metal ions (50 μM). The dark bars represent the response of Schiff-SBA-15 in the presence of the cation of interest. The light bars represent the response upon addition of 50 μM of Cu^{2+} to a solution of Schiff-SBA-15 and the cation of interest. F_0 corresponds to the emission of Schiff-SBA-15 without cation. $\lambda_{ex} = 268$ nm and $\lambda_{em} = 476$ nm.

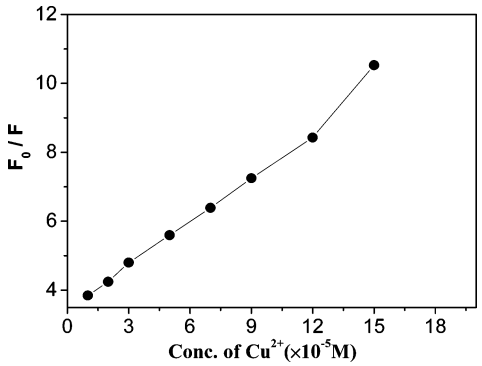

Figure 8. Stern−Volmer plots for the quenching of 0.1 g/L Schiff-SBA-15 by Cu^{2+}.

Stern-Volmer Analysis. The nature of the quenching process is explored by Stern−Volmer analysis. Plotting relative emission intensities (F, F_0) against quencher concentration [Q] for static processes should yield a linear Stern−Volmer plot that describes the static quenching process. From these data the dynamic or static nature of the quenching processes can be determined. In this analysis, the intensity (F, F_0) is plotted vs concentration of quencher ions [Q], according to eq 1. The slope of the line is equivalent to k_d, the rate of dynamic quenching.[47] In a lifetime-based Stern−Volmer plot, when k_d is positive, the quenching is considered dynamic. When k_d is zero, no dynamic quenching can be measured, and emission is quenched by a static mechanism.

$$(F_0/F) = 1 + k_d[Q] \quad (1)$$

$$(F_0/F) = 1 + k_{sv}[Q] \quad (2)$$

Figure 8 indicates the steady-state emission Stern−Volmer analysis for Cu^{2+}−fluorophore interaction in ethanol/water solution, plotted as in eq 2. The data for Cu^{2+} show the very strong quenching from the solution of Schiff-SBA-15, with Cu^{2+} inducing the strongest response. The fluorescence

(45) Métivier, R.; Leray, I.; Lebeau, B.; Valeur, B. *J. Mater. Chem.* **2005**, *15*, 2965.
(46) Casasus, R.; Marcos, M. D.; Martinez-Manez, R.; Ros-Lis, J. V.; Soto, J.; Villaescusa, L. A.; Amoros, P.; Beltran, D.; Guillem, C.; Latorre, J. *J. Am. Chem. Soc.* **2004**, *126*, 8612.
(47) Lakowicz, J. R. *Principles of Fluorescence Spectroscopy*; Plenum Press: New York, 1983.

quenching of Schiff-SBA-15 by the copper ions is most likely caused by energy or electron-transfer reactions between the donor sites of the fluorophore and binding metal complexes, which is a nonradiative center and traps the excitation energy passing through them. This proves the inference we gained from the former spectrums. It is conclusive that for the Cu^{2+}−Schiff-SBA-15 a static quenching mechanism is in effect,[48,49] which results from complexation of the analyte to the receptor sites. Analysis of Stern−Volmer plots in this regime yields equilibrium expressions for static quenching, k_{sv}, which are analogous to associative binding constants for the quencher−acceptor system. A quantified fluorescence quenching ability (k_{sv}) of copper ion to the solutions of Schiff-SBA-15 is obtained from Stern−Volmer quenching curves, which is calculated to be $\log k_{sv} = 4.16$. This suggests that the Cu^{2+} exhibits a strong binding ability with the fluorophore of Schiff-SBA-15.

(48) Murphy, C. B.; Zhang, Y.; Troxler, T.; Ferry, Vn.; Martin, J. J.; Jones, W. E. *J. Phys. Chem. B* **2004**, *108*, 1537.
(49) Zhang, M.; Lu, P.; Ma, Y. G.; Shen, J. C. *J. Phys. Chem. B* **2003**, *107*, 653.

Conclusion

New inorganic−organic hybrid mesoporous SBA-15-type material has been successfully synthesized by co-condensation of TEOS and chelate ligand in the presence of P123 template. And the fluorescence chemosensor described here displays the outstanding sensitivity and selectivity. This method allows the introduction of organic fluorophore with the preservation of uniform mesoscale channels, high specific surface areas, and large pore volumes. The hybrid material can also overcome the technical problems in the use of sensing metal ions in solution, promising a bright future for mesoporous silica encapsulated Schiff base complexes.

Acknowledgment. Financial support from NHTRDP973 (2007CB613301), NSF of China (20773601, 20673053, 20373024, and 20528302), JPNSF (BK2006718, BK2006127, and BG2006030), British American Tobacco (BAT), and Analysis Center and Scientific Research Foundation of Graduate School of Nanjing University is gratefully acknowledged.

IC7008732